# A Dyadic Green's Function for the Plano-Concave Quasi-Optical Resonator

P. L. Heron, F. K. Schwering, *Fellow, IEEE*, G. P. Monahan, *Student Member, IEEE*, J. W. Mink, *Fellow, IEEE*, and M. B. Steer, *Senior Member, IEEE*

***Abstract*—An approximate dyadic Green's function is derived for a quasi-optical resonator. The Green's function is comprised of resonant and nonresonant terms corresponding to coupling to the modal and nonmodal resonator fields. The effect of losses due to diffraction, finite reflector conductivity and radiation are included. Experimental one- and two-port measurements of antennas in an X-band cavity compare favorably with theoretical predictions.**

## I. Introduction.

An approximate dyadic Green's function, $\bar{G}e_c$, is developed which is suitable for use in the design and analysis of cavity type quasi-optical power combiners. Fig. 1 depicts the resonator which consists of an infinite, perfectly conducting plane located at $z = 0$, and a partially transparent shallow spherical reflector which intersects the $z$-axis at $z = D$ and has a rectangular aperture of dimensions $2a_x$ and $2a_y$. $\bar{G}e_c$ is determined by separately considering the resonant cavity modal fields, and nonresonant fields so that

$$\bar{G}e_c = \bar{G}e_r + \bar{G}e_n \tag{1}$$

where the subscripts $r$ and $n$ refer to resonant and nonresonant fields respectively. $\bar{G}e_r$ is determined using the approach of [1] generalized for arbitrary resonator spacing and operating frequency. $\bar{G}e_n$ is found using a half space Green's function, $\bar{G}e_h$, then considering the field components which cannot couple into cavity modes.

## II. Resonant Fields

### A. Beam Modes

The resonant electric fields within the cavity are to be the superposition of a diverging modal wavebeam traveling in the $\hat{\boldsymbol{a}}_z$ direction ($\boldsymbol{E}^+_{mn}$) and a converging modal wavebeam traveling in the $-\hat{\boldsymbol{a}}_z$ direction ($\boldsymbol{E}^-_{mn}$). Assuming that all resonator dimensions are large compared with a wavelength, that $D^2/a^2 \gg N$ holds for both $a = a_x$ and $a = a_y$, and that the Fresnel number $N = a^2/(D\lambda)$ is sufficiently large, the traveling wavebeams can be expressed as Hermite–Gaussian functions for rectangular apertures [2]:

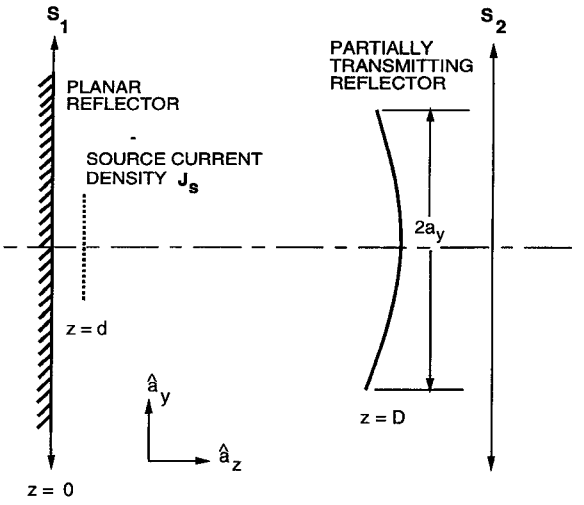


Fig. 1. Cross-section of the Plano-concave resonator.

$$\begin{aligned} E^{\pm}_{mn}(x,y,z) &= \frac{(\mu/\epsilon)^{1/4}}{\sqrt{\pi \bar{X}\bar{Y} m!n!}}(1+u^2)^{-1/4} \\ &\quad (1+v^2)^{-1/4} He_m(\sqrt{2}x/x_z) He_n(\sqrt{2}y/y_z) \\ &\quad \cdot \exp\left\{-\frac{1}{2}\left[(x/x_z)^2 + (y/y_z)^2\right]\right. \\ &\qquad \mp \jmath\left[kz + \frac{1}{2}\left(u(x/x_z)^2 + v(y/y_z)^2\right)\right. \\ &\qquad\quad -\left(m+\frac{1}{2}\right)\tan^{-1}(u) \\ &\qquad \left.\left. -\left(n+\frac{1}{2}\right)\tan^{-1}(v)\right]\right\}, \end{aligned} \tag{2}$$

where the Hermite polynomials are defined by

$$He_n(X) = (-1)^n \exp(X^2/2)\frac{d^n}{dX^n}\left(\exp(-X^2/2)\right) \tag{3}$$

and

$$u = \frac{z}{k\bar{X}^2}, \quad v = \frac{z}{k\bar{Y}^2},$$

$$x_z^2 = \bar{X}^2(1+u^2), \quad y_z^2 = \bar{Y}^2(1+v^2),$$

Manuscript received April 6, 1993. This work was supported in part by the U.S. Army Research Office through grant DAAL03-89-D-0030.

P. L. Heron, G. P. Monahan, and M. B. Steer are with the High Frequency Electronics Laboratory, Department of Electrical and Computer Engineering, North Carolina State University, Raleigh, NC 27695-7911.

F. W. Schwering is with CECOM, Attn. AMSEO-RD-C3-D, Ft. Monmouth, NJ 07703-5203.

J. W. Mink is with the United States Army Research Office, P.O. Box 12211, Research Triangle Park, NC 27709-2211.

IEEE Log Number 9210805.

$$\bar{X}^2 = \frac{1}{k}\sqrt{\left(F_x D\left(2 - \frac{D}{F_x}\right)\right)},$$
$$\bar{Y}^2 = \frac{1}{k}\sqrt{\left(F_y D\left(2 - \frac{D}{F_y}\right)\right)}.$$

In these expressions $F_x$, $F_y$ are the focal lengths of the concave reflector due to curvature along the $x$ and $y$ axes, respectively, and $k$ is the free space wavenumber [3]. The wave beam modes are normalized and in any constant $z$ plane satisfy the orthogonality condition

$$\sqrt{\frac{\epsilon}{\mu}}\int_S E_{st}^{\pm} E_{mn}^{\mp} dS = \mp\delta_{sm}\delta_{tn}. \tag{4}$$

### *B. Cavity Resonant Fields*

Boundary conditions are applied at the reflector surfaces to determine the form of the cavity modal resonant fields. The planar reflector is assumed to be perfectly conducting so that $\hat{\boldsymbol{a}}_z \times \boldsymbol{E} = 0$ at $z = 0$. The spherical reflector is characterized by a reflection coefficient $R_{mn}$ and a transmission coefficient $T_{mn}$ for the $mn$ th Hermite–Gaussian beam mode. Resonant transverse fields excited by a source current are expressed as a series of these modal fields with the coefficients determined by use of the Lorentz reciprocity theorem and an applied test field. This test field consists of a single mode wave beam with polarization components in both the $\hat{\boldsymbol{a}}_x$ and $\hat{\boldsymbol{a}}_y$ directions which converges on the cavity from $z > D$. The transverse modal test fields are

$$\boldsymbol{E}_{T,st} = \begin{cases} \boldsymbol{c}_{st}(E_{st}^{-} - E_{st}^{+}), & 0 < z < D, \\ \hat{\boldsymbol{a}}_T E_{st}^{-} + \boldsymbol{b}_{st} E_{st}^{+}, & z > D. \end{cases} \tag{5}$$

The coefficients $\boldsymbol{c}_{st} = c_{st}^{(x)}\hat{\boldsymbol{a}}_x + c_{st}^{(y)}\hat{\boldsymbol{a}}_y$, $\boldsymbol{b}_{st} = b_{st}^{(x)}\hat{\boldsymbol{a}}_x + b_{st}^{(y)}\hat{\boldsymbol{a}}_y$, and $\hat{\boldsymbol{a}}_T = \hat{\boldsymbol{a}}_x + \hat{\boldsymbol{a}}_y$ for each of the regions are related through the boundary conditions at the spherical reflector. It can be shown that

$$\boldsymbol{c}_{st} = \frac{T_{st}\hat{\boldsymbol{a}}_T}{1 + R_{st}\psi_{st}} \tag{6}$$

and

$$\boldsymbol{b}_{st} = \left(\frac{R_{st}}{\psi_{st}} - \frac{T_{st}^2}{1 + R_{st}\psi_{st}}\right)\hat{\boldsymbol{a}}_T, \tag{7}$$

where $\psi_{st} = E_{st}^{+}/E_{st}^{-}$ is evaluated at the surface of the spherical reflector. Since at $z = D$ the phase fronts of all modes correspond approximately to the surface of the spherical reflector [2], $\psi_{st}$ is evaluated at $\{x, y, z\} = \{0, 0, D\}$.

The resonant source fields excited by a current density $\boldsymbol{J}_S$ in the $z = d$ plane are expressed as the series

$$\boldsymbol{E}_S = \sum_{mn}\begin{cases} \boldsymbol{f}_{mn}(E_{mn}^{-} - E_{mn}^{+}), & 0 \le z < d, \\ \boldsymbol{a}_{mn}(E_{mn}^{-} - (1 + \varepsilon_{mn})E_{mn}^{+}), & d < z \le D, \\ \boldsymbol{g}_{mn}E_{mn}^{+}, & z > D, \end{cases} \tag{8}$$

and the fields $\boldsymbol{H}_T$ and $\boldsymbol{H}_S$ are found using

$$\boldsymbol{H}_{mn}^{\pm} = \pm\sqrt{\frac{\epsilon}{\mu}}\hat{\boldsymbol{a}}_z \times \boldsymbol{E}_{mn}^{\pm}. \tag{9}$$

Using the boundary conditions at the spherical reflector as well as requiring continuity of the field at $z = d$ on a mode by mode basis, the expansion coefficients of $\boldsymbol{E}_S$ for the various regions are related by

$$(1 + \epsilon_{mn}) = -\frac{1}{R_{mn}\psi_{mn}},$$
$$\boldsymbol{a}_{mn} = \boldsymbol{g}_{mn}\frac{R_{mn}\psi_{mn}}{T_{mn}},$$
$$\boldsymbol{f}_{mn} = \boldsymbol{a}_{mn}\frac{\left(1 - \frac{\Upsilon_{mn}}{R_{mn}\psi_{mn}}\right)}{1 - \Upsilon_{mn}}, \tag{10}$$

where $\Upsilon_{mn} = E_{mn}^{+}/E_{mn}^{-}$ is evaluated at $\{x, y, z\} = \{0, 0, d\}$. The unknown coefficients of (8) can now be determined using $\boldsymbol{E}_{T,st}$ and the Lorentz reciprocity theorem.

### *C. Application of Reciprocity Theorem*

The Lorentz reciprocity theorem is now applied over the volume $\boldsymbol{\Omega}$ which is bounded by the surface $\boldsymbol{S} = S_1 + S_2$ as shown in Fig. 1. For this situation, the Lorentz integral is

$$\oint_S (\boldsymbol{E}_T \times \boldsymbol{H}_S - \boldsymbol{E}_S \times \boldsymbol{H}_T)\cdot\hat{\boldsymbol{n}}dS = -\int_{\boldsymbol{\Omega}} \boldsymbol{E}_T \cdot \boldsymbol{J}_s dV. \tag{11}$$

Since $\hat{\boldsymbol{a}}_z \times \boldsymbol{E} = 0$ at $z = 0$, the integral on $\boldsymbol{S}_1$ vanishes. Using (4) with (5), (8), and (9), the integral over $\boldsymbol{S}_2$ reduces to

$$\sqrt{\frac{\epsilon}{\mu}}\sum_{mn}\int_{S_2}\left[E_{mn}^{+}E_{st}^{-}\hat{\boldsymbol{a}}_T \times (\hat{\boldsymbol{a}}_z \times \boldsymbol{g}_{mn}) + E_{mn}^{+}E_{st}^{-}\boldsymbol{g}_{st} \times (\hat{\boldsymbol{a}}_z \times \hat{\boldsymbol{a}}_T)\right]\cdot\hat{\boldsymbol{a}}_z dS. \tag{12}$$

Since the $\hat{\boldsymbol{a}}_x$ component of $\boldsymbol{J}_S$ produces an $\hat{\boldsymbol{a}}_x$ polarized electric field and the $\hat{\boldsymbol{a}}_y$ component of $\boldsymbol{J}_S$ produces an $\hat{\boldsymbol{a}}_y$ polarized electric field, (11) and (12) result in

$$\boldsymbol{g}_{mn} = \frac{T_{mn}}{2(1 + R_{mn}\psi_{mn})}\int_{\boldsymbol{\Omega}}(E_{mn}^{+} - E_{mn}^{-})\bar{\boldsymbol{I}}_T \cdot \boldsymbol{J}_s dV, \tag{13}$$

where $\bar{\boldsymbol{I}}_T = \hat{\boldsymbol{a}}_x\hat{\boldsymbol{a}}_x + \hat{\boldsymbol{a}}_y\hat{\boldsymbol{a}}_y$.

---

$$\bar{\boldsymbol{G}}\boldsymbol{e}_r = \sum_{mn}\begin{cases} -\frac{(R_{mn}\psi_{mn} + \Upsilon_{mn})}{2(1 - \Upsilon_{mn})(1 + R_{mn}\psi_{mn})}(E_{mn}^{-} - E_{mn}^{+})(\acute{E}_{mn}^{-} - \acute{E}_{mn}^{+})\bar{\boldsymbol{I}}_t, & 0 < z < d, \\ -\frac{R_{mn}\psi_{mn}}{2(1 + R_{mn}\psi_{mn})}\left(E_{mn}^{-} + \frac{E_{mn}^{+}}{R_{mn}\psi_{mn}}\right)(\acute{E}_{mn}^{-} - \acute{E}_{mn}^{+})\bar{\boldsymbol{I}}_t, & d < z < D, \\ -\frac{T_{mn}}{2(1 + R_{mn}\psi_{mn})}E_{mn}^{+}(\acute{E}_{mn}^{-} - \acute{E}_{mn}^{+})\bar{\boldsymbol{I}}_t, & D < z, \end{cases} \tag{14}$$

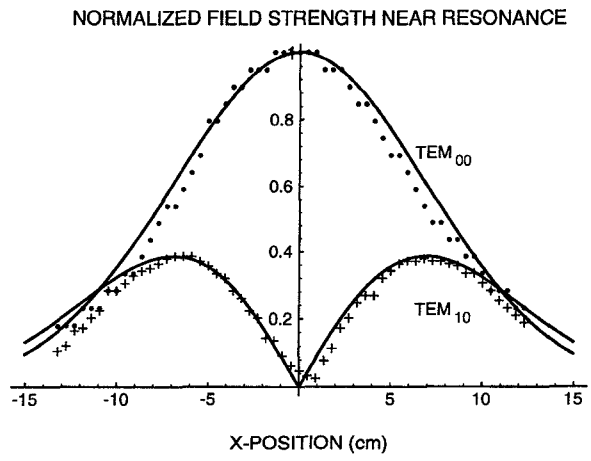


Fig. 2. Comparison of theoretical (line) and measured (points) modal field distribution for the $TEM_{00}$ and $TEM_{01}$ modes along the line $y = -13.2$ cm.

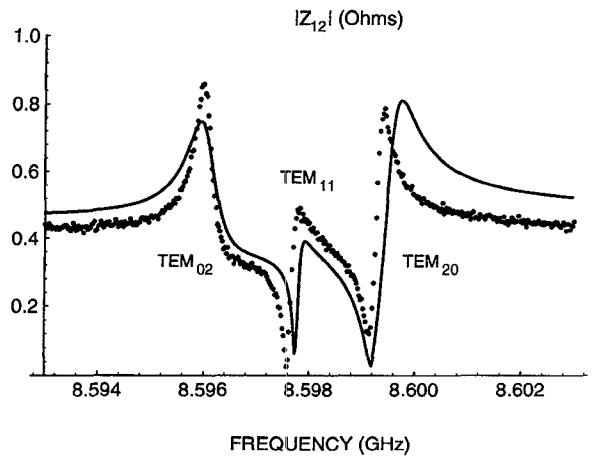


Fig. 3. Predicted (line), using (17), and measured (points) impedance for two inverted-$L$ antennas in a Plano-concave resonator.

## III. Green's Function

The cavity resonant fields are expressed by combining (8), (10), and (13). The resonant Green's function is then written from the resulting expression as (14) (see (14) at the bottom of p. 257) where $\acute{E}^{\pm}_{mn}$ is a function of the source coordinate system $\acute{\boldsymbol{r}} = \{\acute{x}, \acute{y}, \acute{z}\}$, and $E^{\pm}_{mn}$ is a function of the observation coordinate system $\boldsymbol{r} = \{x, y, z\}$.

Conductor losses and mode diffraction losses are included in (14) by perturbing the value of $R_{mn}$. Diffraction losses are computed using the method proposed by Soohoo [4] in which an integral equation for the resonator is formulated by use of Huygen's principle, then solved numerically to determine a modal beam transit gain. Losses due to finite conductivity of metallic reflectors are computed using surface resistance calculations. The conductor losses at the planar reflector are also lumped into the characteristics of the spherical reflector. Equation (14) is modified by multiplying $R_{mn}$ by the modal transit gain and conductor reflection coefficient.

The nonresonant field term, $\bar{\boldsymbol{G}}e_n$, is derived by assuming that the nonresonant field structure near the plane $z = d$ is essentially unchanged if the spherical reflector is removed. The half-space bounded by an infinite conducting plane has a Green's function

$$\frac{\bar{\boldsymbol{G}}e_h}{j\omega\mu_0} = \left(\bar{I} - \frac{\nabla\acute{\nabla}}{k_0^2}\right)(G_0(\boldsymbol{r};\acute{\boldsymbol{r}}) - G_0(\boldsymbol{r};\acute{\boldsymbol{r}} - 2\acute{z}\hat{\boldsymbol{a}}_z)) + 2G_0(\boldsymbol{r};\acute{\boldsymbol{r}} - 2\acute{z}\hat{\boldsymbol{a}}_z)\hat{\boldsymbol{a}}_z\hat{\boldsymbol{a}}_z, \quad (15)$$

where

$$G_0(\boldsymbol{r};\acute{\boldsymbol{r}}) = \frac{\exp(jk|\boldsymbol{r} - \acute{r}|)}{4\pi|\boldsymbol{r} - \acute{r}|}, \text{ and } \bar{I} = \hat{\boldsymbol{a}}_x\hat{\boldsymbol{a}}_x + \hat{\boldsymbol{a}}_y\hat{\boldsymbol{a}}_y + \hat{\boldsymbol{a}}_z\hat{\boldsymbol{a}}_z.$$

$\bar{\boldsymbol{G}}e_h$ includes coupling into paraxial Hermite–Gaussian traveling wave beams that would become resonant modal fields in the presence of the curved reflector. This component, $\bar{\boldsymbol{G}}e_p$, is removed from $\bar{\boldsymbol{G}}e_h$ to produce $\bar{\boldsymbol{G}}e_n$. $\bar{\boldsymbol{G}}e_p$ is found using

$$\bar{\boldsymbol{G}}e_p = \lim_{R_{mn}\to 0} \bar{\boldsymbol{G}}e_r. \quad (16)$$

Thus, the complete Green's function for the interior of the cavity is expressed using (1) as

$$\bar{\boldsymbol{G}}e_c = \bar{\boldsymbol{G}}e_h - \sum_{mn} \frac{R_{mn}\psi_{mn}}{2(1 + R_{mn}\psi_{mn})} \cdot(E^{-}_{mn} - E^{+}_{mn})(\acute{E}^{-}_{mn} - \acute{E}^{+}_{mn})\bar{I}_t, \qquad 0 < z < D. \quad (17)$$

## IV. Results and Conclusion

The validity of (17) was investigated by comparing measured field-strength with that predicted by theory. An X-band cavity was fed through the planar reflector by a short inverted-L antenna. The resonant fields were mapped by studying changes in the antenna reflection coefficient as a function of the position of a small lossy sphere in the $z = 40$ mm plane. Fig. 2 shows a comparison of the measured field profile with that predicted by $\bar{\boldsymbol{G}}e_r$ near resonance. The antenna is electrically short and is treated as a point source. Verification of the complete Green's function was performed by taking calibrated two-port measurements for two inverted-L antennas in the resonator. The theoretical impedance $Z_{12}$ for the two antennas in the cavity was computed using (17) and showed good agreement with measurements. Fig. 3 shows typical results comparing measured and calculated values of $|Z_{12}|$.

In conclusion, the dyadic Green's function represents the resonant and nonresonant fields excited by a current density and may be used in the design of probe or antenna excited quasi-optical cavities and Gaussian waveguiding systems.

## References

[1] J. W. Mink, "Quasi-optical power combining of solid-state millimeter-wave sources," *IEEE Trans. Microwave Theory Tech.*, vol. MTT-34, pp. 273–279, Feb. 1986.

[2] G. D. Boyd and J. P. Gordon, "Confocal multimode resonator theory for millimeter through optical wavelength masers," *Bell Syst. Tech. J.*, vol. 40, pp. 489–509, Mar. 1961.

[3] G. Goubau, "Beam waveguides," *Advances in Microwaves*. New York: Academic Press, 1968, vol. 3, pp. 67–126.

[4] R. F. Soohoo, "Nonconfocal multimode resonators for masers," *Proc. IEEE*, vol. 51, pp. 70–75, Jan. 1963.